Small clusters with Heisenberg antiferromagnetic exchange

2000 J. Phys.: Condens. Matter 12 8669

(http://iopscience.iop.org/0953-8984/12/40/311)

J. Phys.: Condens. Matter **12** (2000) 8669–8682. Printed in the UK PII: S0953-8984(00)15308-1

Small clusters with Heisenberg antiferromagnetic exchange

J B Parkinson† and J Timonen‡

† Department of Mathematics, UMIST, PO Box 88, Manchester M60 1QD, UK
‡ Department of Physics, University of Jyväskylä, PO Box 35, FIN-40351 Jyväskylä, Finland

Received 6 July 2000

Abstract. We study small symmetrical clusters of magnetic ions with Heisenberg antiferromagnetic exchange interaction. We calculate the magnetization and the specific heat as functions of applied magnetic field at zero and non-zero temperature. Results are given for both classical and quantum systems. At zero temperature the classical systems undergo a series of transitions where the symmetry changes as a function of applied field. The quantum systems show similar features to Ising systems previously studied.

1. Introduction

Ten years ago Stern–Gerlach-type experiments were first used to measure the magnetic properties of small atomic clusters [1, 2]. It soon became evident that small clusters of Fe and Co atoms behave at low, but not too low, temperatures as superparamagnets [3, 4]. As the anisotropy energies of these clusters are not very high, above the 'blocking temperature' their total magnetic momenta will turn in a Stern–Gerlach magnetic field via exchange of angular momentum with the rotational degrees of freedom of the clusters. Most of the observed magnetic properties of small ferromagnetic clusters could be attributed to this kind of superparamagnetic behaviour. Some observations, notably that of the increasing magnetization with increasing temperature of very small Fe clusters, have, however, remained controversial to date. Obviously similar experiments would be difficult to do on antiferromagnetic clusters even when they have a small non-zero magnetization due to unpaired spins.

Recently another way of producing magnetic 'clusters' has attracted great interest. These clusters are formed by magnetic ions inside a large molecule of otherwise non-magnetic atoms. A crystal can then be formed in which the magnetic molecules are embedded in a non-magnetic matrix such that there is essentially no magnetic interaction between different molecules. Because there are large numbers of identical, non-interacting molecules, the properties of individual molecules can be easily studied. The observed magnetic properties are therefore determined by the strong exchange interactions between the magnetic ions in the molecule together with terms resulting from structural anisotropy.

The most commonly studied of these materials is $Mn_{12}O_{12}(CH_3COO)_{16}(H_2O)_4$ in which the cluster is a group of twelve Mn atoms. This group contains a central tetrahedron of Mn^{4+} ($S = 3/2$) atoms and eight Mn^{3+} ($S = 2$) atoms arranged around it. The exchange interactions cause the central atoms to point parallel to each other with the outer atoms all pointing in the opposite direction, giving a ground state with $S = 10$. In fact these magnetic molecules behave very much as the superparamagnets formed by small ferromagnetic clusters described

0953-8984/00/408669+14$30.00

above [5–12]. One of the most interesting features of these molecules has been the relaxation of their magnetic moments when the external magnetic field is reversed.

Another widely studied material is Fe_8-triazacyclononane, in which the magnetic cluster is an arrangement of eight Fe atoms [13–17]. Again the behaviour is superparamagnetic.

Clearly these particular molecules are not examples of antiferromagnetic clusters but they do indicate that chemists can now construct materials with large numbers of identical clusters with clearly defined symmetry and interesting magnetic properties. It seems likely that similar materials with antiferromagnetic clusters could be constructed.

On the other hand, there is very recent theoretical evidence that in small atomic clusters the sign of the effective exchange interaction between adjacent spins can vary, depending on the size and geometry of the cluster [18–21]. It is thus possible that interesting magnetic properties could still be found for very small atomic clusters which have not so far been investigated experimentally.

Although the properties of small ferromagnetic clusters of atoms are now well understood, much less is known about antiferromagnetic clusters. Only the extreme anisotropic limit in which the interaction is Ising-like has been studied [22]. Their magnetization as a function of applied field has been studied together with some effects caused by surface spins and lattice distortions. Many of these systems are frustrated since their structures are such that they contain triangles of nearest-neighbour spins. One might expect that Heisenberg exchange rather than Ising exchange would introduce differences, some of which could be significant and, in any case, Heisenberg interactions are more realistic. A study of the classical ground states of these systems, which are not obvious except at large applied fields, could also be useful in dealing with systems with large spin which cannot be easily handled quantum mechanically. Consequently, we feel that numerical and analytic studies of the zero- and low-temperature behaviour of small antiferromagnetic clusters are worthwhile.

In this paper we study the small clusters shown in figure 1.

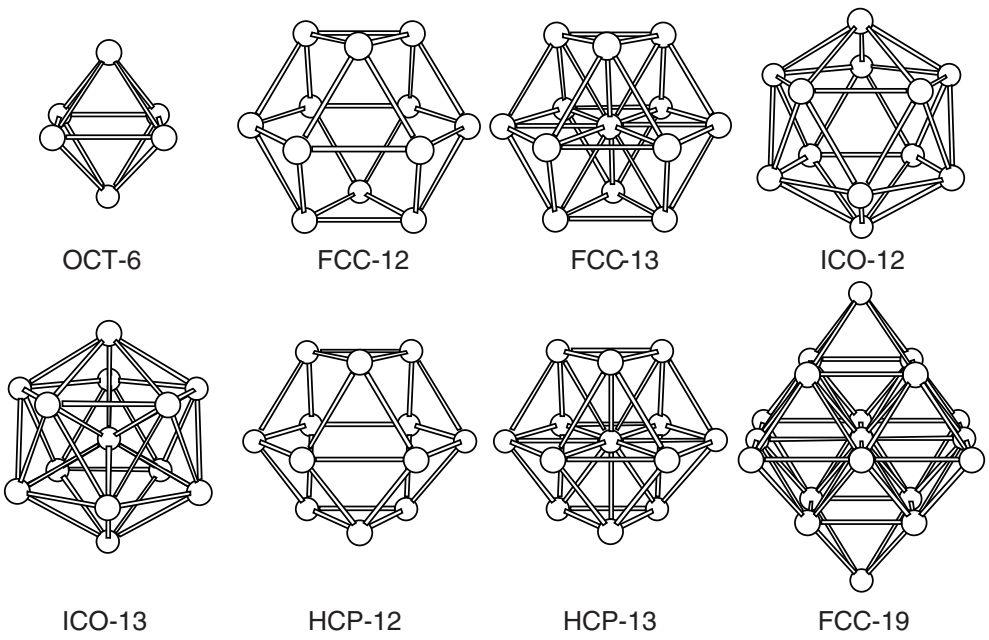

Figure 1. The eight clusters studied in this paper.

We assume that all interactions are nearest neighbour and are antiferromagnetic with the same strength. The Hamiltonian is the usual Heisenberg interaction

$$H = B\sum_i S_i^z + J\sum_{\langle i,j\rangle} \boldsymbol{S}_i \cdot \boldsymbol{S}_j \tag{1}$$

where $\langle i, j\rangle$ are all nearest-neighbour pairs of magnetic atoms. J is the antiferromagnetic exchange interaction which will be put equal to +1 from now on. The spin $S = \frac{1}{2}$.

2. Classical properties

At zero temperature the classical system is in its ground state, the configuration with lowest energy. The exchange energy associated with a bond is given by $e_{ij} = \boldsymbol{S}_i \cdot \boldsymbol{S}_j$ which in terms of the polar angles θ_i, ϕ_i of the two atoms can be written as

$$e_{ij} = S^2(\cos(\theta_i)\cos(\theta_j) + \sin(\theta_i)\sin(\theta_j)\cos(\phi_i - \phi_j)) \tag{2}$$

and the magnetic energy for each atom is $BS\cos(\theta_i)$ giving a total energy

$$E = \sum_{\langle i,j\rangle} e_{ij} + BS\sum_i \cos(\theta_i). \tag{3}$$

For a cluster of N atoms this is a function of $2N$ variables. The minimum energy can be found numerically using standard techniques. We used a Powell method [23], in which the directions along which minimization takes place in the multi-dimensional space are chosen in an optimal manner. Once the minimum-energy configuration is known, the magnetization

$$M = S\sum_i \cos(\theta_i)$$

can be calculated. We also investigate the susceptibility $\mathrm{d}M/\mathrm{d}B$.

At very high B all the atoms are aligned parallel to the field. For the clusters with a single central atom, reducing B first causes the central atom to rotate until it is antiparallel with the other atoms. During this process the remaining atoms rotate a small amount away from the z-direction. There is then a plateau of constant magnetization. Then the parallel alignment of the atoms on the outer shell(s) starts to break down. This may happen in more than one phase with different symmetries and well-defined transitions between them.

From the numerical solutions we could determine the symmetry of the configurations. This enables the energy to be written as a function of only two or three of the variables. In some cases we could then solve the non-linear equations and explicitly determine the equation of the M–B curve. We could also sometimes determine analytically the crossover fields to states of different symmetry. In the following results these fields are given by algebraic values. However, this was not always possible, and then the M–B curve and the crossover points had to be determined numerically, albeit as accurately as desired.

2.1. OCT-6

There are two regions.

(a) $0 < B \leqslant 3$. The magnetization is given by $M = B$ with constant susceptibility $\chi = 1$. The ground state in this region is highly degenerate. Spins on opposite corners of the octahedron are parallel, and for each nearest-neighbour triangle the total spin of the three atoms, $\boldsymbol{S}_{tri}$, is given by $S_{tri}^x = S_{tri}^y = 0$, $S_{tri}^z = M/2$.

(b) $B \geqslant 3$. The magnetization is $M = 3$ with all the spins aligned parallel to the field.

2.2. FCC-12

There are two regions.

(a) $0 < B \leqslant 3$. The magnetization is given by $M = 2B$ with constant susceptibility $\chi = 2$. The ground state in this region is highly degenerate. Spins on opposite corners of each square face of the cluster are parallel, and for each nearest-neighbour triangle the total spin of the three atoms, $\boldsymbol{S}_{tri}$, is given by $S^x_{tri} = S^y_{tri} = 0$, $S^z_{tri} = M/2$.

(b) $B \geqslant 3$. The magnetization is $M = 6$ with all the spins aligned parallel to the field.

2.3. FCC-13

There are four regions.

(a) $0 < B \leqslant 2.5$. The magnetization is given by $M = 0.5 + 2B$. In this region for each nearest-neighbour triangle the total spin of the three atoms, $\boldsymbol{S}_{tri}$, is given by $S^x_{tri} = S^y_{tri} = 0$, $S^z_{tri} = (M + 0.5)/4$.

(b) $2.5 < B \leqslant 5.5$. The magnetization is constant: $M = 5.5$. Here the central atom is aligned antiparallel to the field, with all other atoms parallel to it.

(c) $5.5 < B \leqslant 6.5$. The magnetization is given by $M = B$. The atoms all lie in the same vertical plane which can be chosen as the xz-plane. Here $\sin(\theta_1) = 12\sin(\theta_2)$ with $\phi_1 = 0$ and $\phi_2 = \pi$, where θ_1, ϕ_1 are the polar angles of the central atom and θ_2, ϕ_2 the polar angles of all the other atoms.

(d) $B > 6.5$. The magnetization is constant: $M = 6.5$.

The first two regions have a similar behaviour to the FCC-12 cluster, except that $M \to 0$ in FCC-12 and $M \to 0.5$ in FCC-13 as $B \to 0$. The magnetization curve for FCC-13 is shown in figure 2.

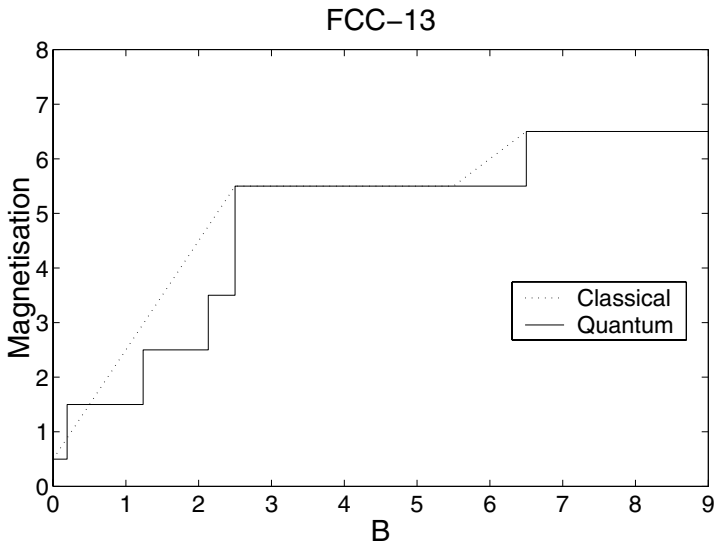

Figure 2. Quantum and classical magnetization at $T = 0$ of the FCC-13 cluster.

2.4. FCC-19

There are six regions.

(a) $0 < B < B_{c1}$ where $B_{c1} \approx 0.9331$. The magnetization increases monotonically from $M \approx 0.2979$ at $B = 0$ to $M \approx 2.18$ at $B = B_{c1}$.

(b) $B_{c1} < B < B_{c2}$ where $B_{c2} \approx 2.7330$. The magnetization is given by $M = \frac{7}{3}B$.

(c) $B_{c2} < B < B_{c3}$, where $B_{c3} = (11 - \sqrt{17})/4 \approx 3.7808$. The magnetization increases monotonically from $M \approx 6.377$ to $M = 8.5$.

(d) $B_{c3} < B < B_{c4}$ where $B_{c4} = (17 + \sqrt{17})/4 \approx 5.2807$. The magnetization is constant at $M = 8.5$.

(e) $B_{c4} < B < B_{c5}$ where $B_{c5} = (19 + \sqrt{57})/4 \approx 6.6375$. The magnetization increases monotonically from $M = 8.5$ to $M = 9.5$.

(f) $B > B_{c5}$. The spins are all aligned parallel to the field and the magnetization is constant at $M = 9.5$.

Figures 3 and 4 show the magnetization and the susceptibility over the whole range.

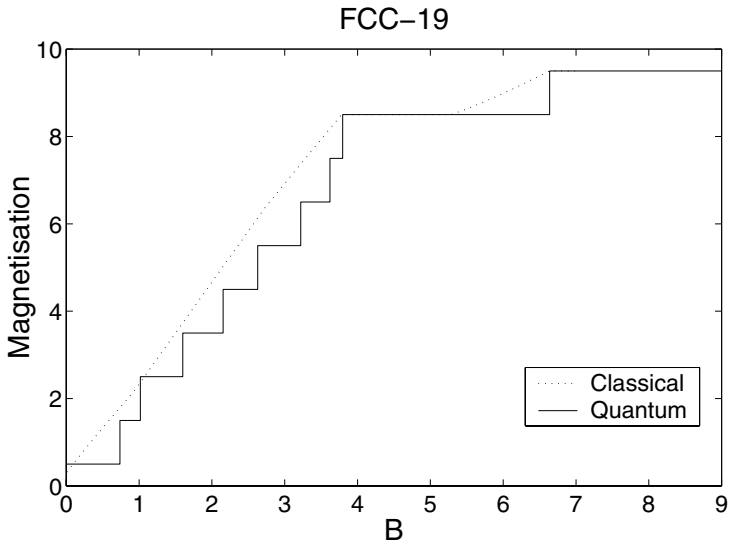

Figure 3. Quantum and classical magnetization at $T = 0$ of the FCC-19 cluster.

2.5. ICO-12

There are three regions.

(a) $0 < B < B_{c1}$ where $B_{c1} \approx 1.470$. The magnetization increases monotonically from $M = 0$ to $M \approx 2.359$.

(b) $B_{c1} < B < B_{c2}$ where $B_{c2} = (5 + \sqrt{5})/2 \approx 3.6180$. The magnetization is given by $M = 1 + 5(2B - 1)/(2B_{c2} - 1)$, with constant susceptibility $\chi = 10/(2B_{c2} - 1)$.

(c) $B > B_{c2}$. The magnetization is constant: $M = 6$, with all spins aligned parallel to the applied field.

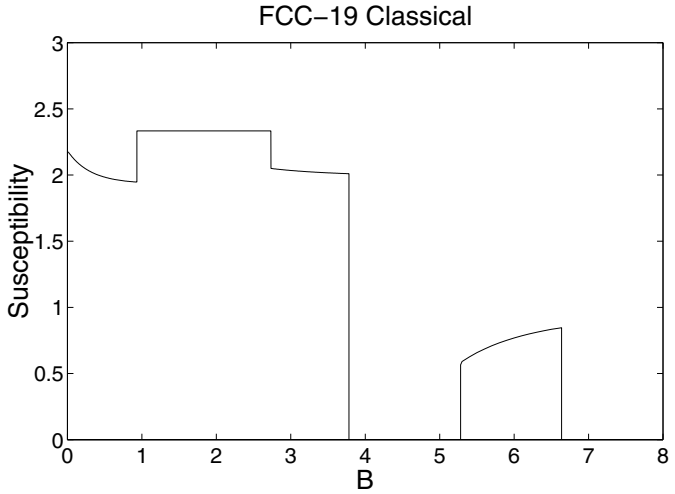

Figure 4. Classical susceptibility at $T = 0$ of the FCC-19 cluster.

2.6. ICO-13

There are five regions.

(a) $0 < B < B_{c1}$ where $B_{c1} \approx 0.969$. The magnetization increases monotonically from $M \approx 0.263$ to $M \approx 1.857$. The symmetry in this region is one in which the twelve shell atoms are arranged in four groups of three. The atoms in each group of three have the same z-component and have equal angular spacing around the z-axis. An analytic formula for M has not been obtained for this region. At B_{c1} there is discontinuity in the magnetization which jumps from $\sim$1.857 to $\sim$2.054.

(b) $B_{c1} < B < B_{c2}$ where $B_{c2} = (4+\sqrt{5})/2 \approx 3.1180$. The magnetization is given by $M = 0.5 + 5B/B_{c2}$, with constant susceptibility $\chi = 5/B_{c2}$. The symmetry in this region is that the central atom and two atoms on opposite corners of the shell point antiparallel to the field, while the remaining atoms all have the same z-component and equal angular spacing around the z-axis.

(c) $B_{c2} < B < 5.5$. The magnetization is constant: $M = 5.5$.

(d) $5.5 < B < 6.5$. The magnetization is given by $M = B$.

(e) $B > 6.5$. The magnetization is constant: $M = 6.5$, with all spins aligned parallel to the applied field.

The first three regions show a marked similarity to the regions observed in the ICO-12 model, with the exception that $M \to 0$ for ICO-12 but $M \to 0.263$ for ICO-13 as $T \to 0$. The magnetization for all five regions is shown in figure 5, and the susceptibility in figure 6.

2.7. HCP-12

This is similar to FCC-12 and again there are two regions.

(a) $0 < B \leqslant B_{c1}$ where $B_{c1} = 3.257\,07$. The magnetization increases monotonically from 0 to 6. The curve is not a straight line and the gradient $\mathrm{d}M/\mathrm{d}B$ decreases from about 1.86 to about 1.81 over the region. The three upper and three lower atoms all have equal z-component and are spaced equally around the z-axis. The six central atoms again have

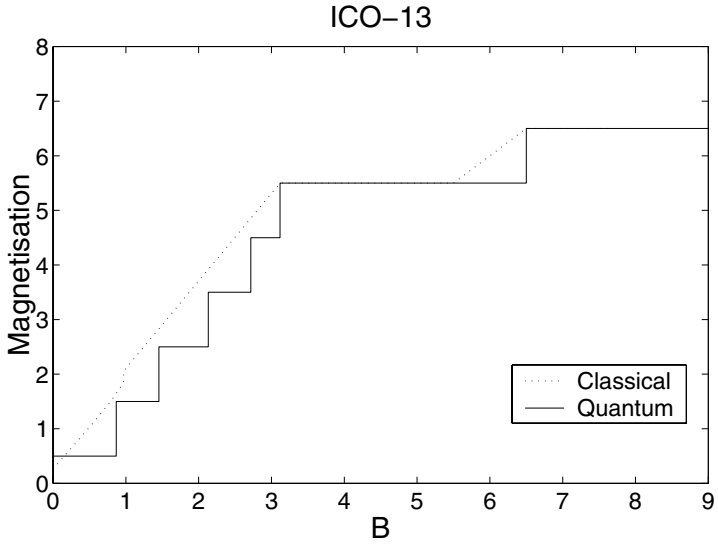

Figure 5. Quantum and classical magnetization at $T = 0$ of the ICO-13 cluster.

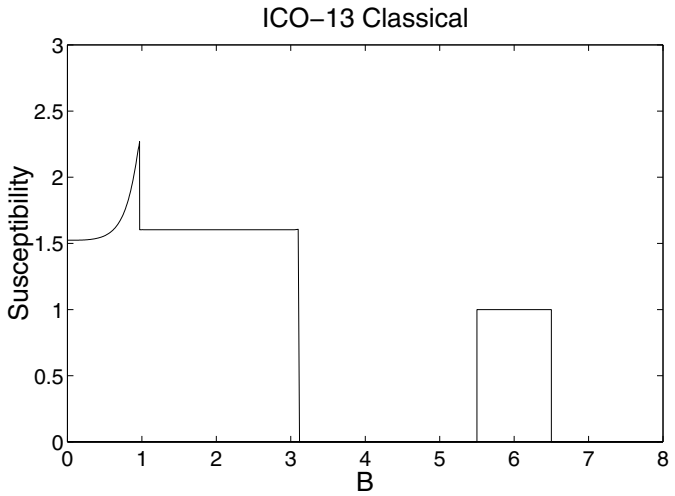

Figure 6. Classical susceptibility at $T = 0$ of the ICO-13 cluster.

equal z-component and are arranged in two groups of three, each of which is spaced equally around the z-axis. As $M \to 0$ all the atoms become oriented perpendicular to $\boldsymbol{B}$. The value of B_{c1} is $3 + \sqrt{3}\cos(2\alpha)$ where α is the solution of

$$\sqrt{3}\cos(3\alpha) + \sin(\alpha) = 0. \tag{4}$$

(b) $B \geqslant B_{c1}$. The magnetization is constant: $M = 6$.

2.8. HCP-13

This is similar to FCC-13 and again there are four regions.

(a) $0 < B \leqslant B_{c1}$ where $B_{c1} = 2.757\,07$. This region is very similar to the corresponding region in HCP-12. The magnetization increases monotonically from M_0 to 5.5 where $M_0 \approx 0.4299$. Again the gradient $\mathrm{d}M/\mathrm{d}B$ decreases from about 1.86 to about 1.81 over the region. The value of B_{c1} is $5/2 + \sqrt{3}\cos(2\alpha)$ where α is the solution of equation (4). The value of M_0 is not known in closed form.

(b) $B_{c1} < B \leqslant 5.5$. The magnetization is constant: $M = 5.5$. Here the central atom is aligned antiparallel to the field, with all other atoms parallel to it.

(c) $5.5 < B \leqslant 6.5$. The behaviour is the same as for FCC-13.

(d) $B > 6.5$. The behaviour is the same as for FCC-13.

3. Quantum ground states

The principal difference between a finite quantum spin system and the corresponding classical system at $T = 0$ is that the quantum system shows a series of discrete steps in the magnetization–field curves. To obtain the quantum curve, the Hamiltonian with $B = 0$ is diagonalized to find all the eigenvalues. Only the lowest eigenvalue for each $S_T^z = M$ is needed. If this is E_M, then the energy as a function of field is $E_M - BM$. As the field increases the energy of a state with a larger value of M will cross that with a lower M and there will be a step in the curve.

The exact pattern of the steps depends on the E_M, but the number of steps is always equal to or less than NS where N is the number of atoms in the cluster and S the spin. We usually observed steps of one unit in these systems although for the FCC-12 and FCC-13 clusters there are larger jumps. Larger jumps are more common in the Ising case as shown by Merikoski *et al* in 1997 [22] and result in fewer than the maximum number of steps.

We are interested to see if the classical results of the previous section can shed any light on the behaviour of the corresponding quantum system. The simplest case is OCT-6 in which the classical magnetization curve is a straight line and the quantum steps have corners lying on this line as shown in figure 7.

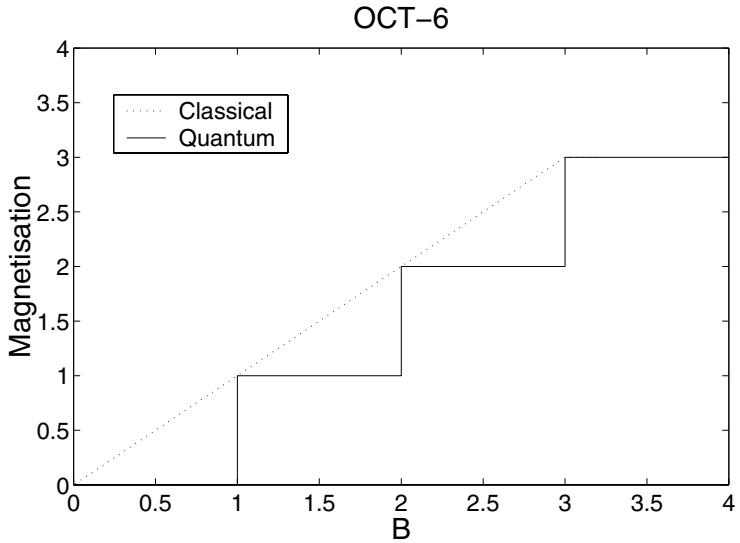

Figure 7. Quantum and classical magnetization at $T = 0$ of the OCT-6 cluster.

For the FCC-12 and FCC-13 clusters the classical magnetization curve is again very simple but we find that the quantum behaviour is more complicated and shows steps of variable width (see figure 2). In both cases there seems to be a region where the width of the steps decreases with increasing field but this behaviour breaks down at low fields. The FCC-13 cluster has a single extra step at high field where the central spin reverses corresponding to the high-field classical region.

The three other systems show a more complicated classical behaviour. Firstly consider the ICO-12 and ICO-13 cases, which are rather similar apart from the extra step at high field for the latter. The lower-field region where the magnetization is changing is in two parts, $0 < B < B_{c1}$ and $B_{c1} < B < B_{c2}$ with different magnetization curves (see figures 5 and 6). A close examination of the quantum magnetization curves shows that the step widths do *not* decrease monotonically. There is a change at a value of B which roughly corresponds to B_{c1}. For the ICO-13 system a very similar behaviour is observed for the lowest two regions, again with a change at roughly $B = B_{c1}$. The steps shown on the quantum curve in figure 5 occur at $B = 0.8681$, 1.4530, 2.1327, 2.7162, 3.1180 and 6.5.

The most complex case is the FCC-19 system, which is to be expected since this has a central atom surrounded by two shells. Again the reversal of the central atom at high field corresponds to a single step at $B = B_{c5}$. At lower fields the three classical regions bounded by $B = 0$, B_{c1}, B_{c2} and B_{c3} appear to correspond roughly to three quantum regions in which the widths decrease monotonically with breaks in the monotonic decrease at similar values of B to the classical case. The curves are shown in figure 3.

We conclude that there is some weak evidence that transitions between states of different symmetry observed in a classical systems may have corresponding transitions in quantum systems, indicated by a change in the trend of the step widths. On the other hand, changes in step width behaviour in the quantum systems do not seem to necessarily indicate that the classical system has a corresponding transition, as the FCC-12 and FCC-13 systems show.

4. Non-zero temperature

Since these systems have small numbers of atoms it is possible in the quantum case to calculate all the eigenvalues and hence the partition function. From this the non-zero temperature properties can be found. A similar calculation is much more difficult for the classical system as it involves integration over $2N$ variables, the orientational angles of the N spins. We have not attempted this, so our results are confined to the quantum systems.

Figures 8 and 9 show the magnetization–B curves for the FCC-13 and ICO-13 systems at various temperatures.

The features are very similar to those of the Ising systems apart from the differences noted in the previous section. In particular, we also find small ranges of B in which the magnetization increases with temperature, although the effect is not so pronounced because there are no large magnetization steps in the ground state.

5. Specific heat

From the partition function Z_0 and the related functions Z_1 and Z_2 of the quantum systems the specific heat can be calculated. The functions are defined by

$$Z_n = \sum_i (E_i)^n \exp(-E_i/T) \tag{5}$$

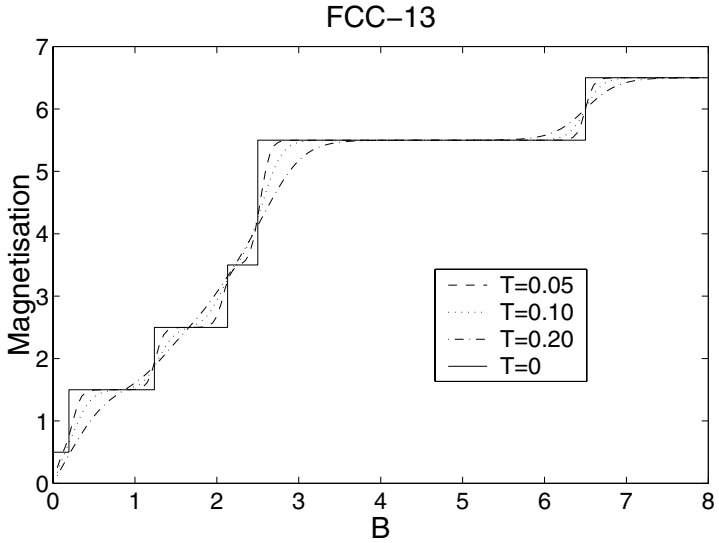

Figure 8. Quantum magnetization at various T of the FCC-13 cluster.

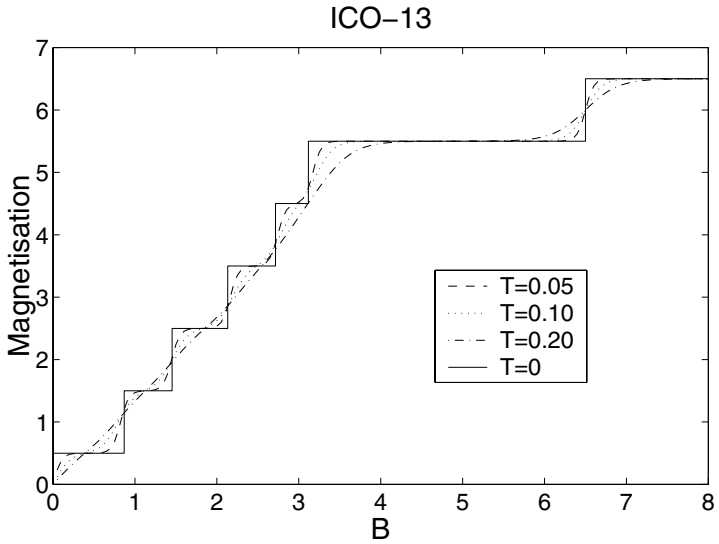

Figure 9. Quantum magnetization at various T of the ICO-13 cluster.

where $\{E_i\}$ are the eigenvalues of the cluster in the presence of the magnetic field B. Z_0 is the usual partition function, and $\langle E\rangle = Z_1/Z_0$ etc.

The specific heat is given by

$$C = \frac{1}{T^2}(\langle E^2\rangle - \langle E\rangle^2) = \frac{1}{T^2}\frac{Z_0 Z_2 - Z_1^2}{Z_0^2}. \tag{6}$$

A plot of C as a function of B and T is shown in figure 10. for the ICO-13 cluster. The specific heats for other clusters show similar features.

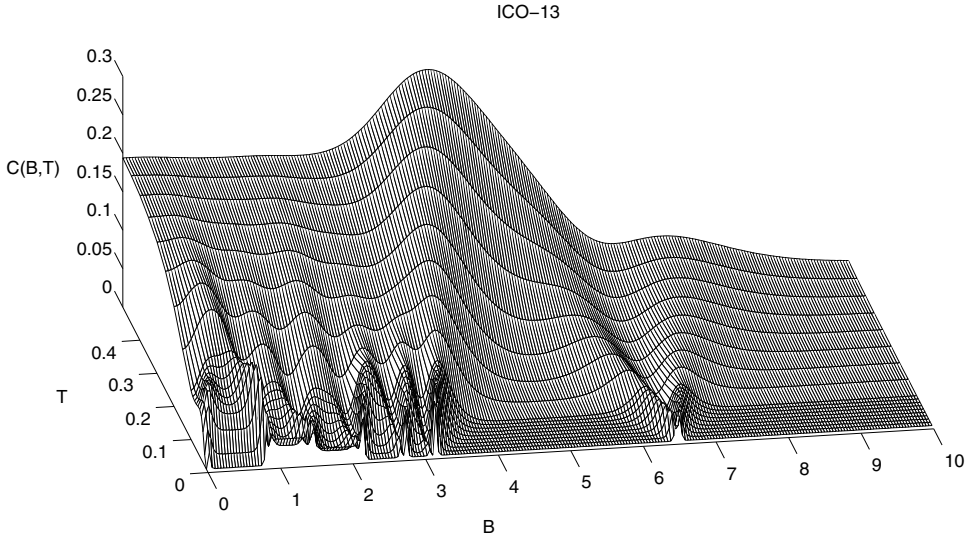

Figure 10. Specific heat per atom as a function of B and T of the ICO-13 cluster.

At low temperatures, $T \ll J$, the specific heat varies rapidly with B, showing a series of double peaks, before tending to 0 at high B where the ground state has all spins aligned with a large gap to the first excited state. The double peaks (most obvious near $B = 6.5$ in the figure) occur at fields where the ground state changes by a crossover of levels. These fields are precisely those at which steps in the $T = 0$ magnetization curves occur. The peaks become very narrow as $T \to 0$ but the height remains finite. The detailed behaviour close to a divergence is rather complicated in general. However, for a system with just two spin-$\frac{1}{2}$ atoms there is a single crossover at $B = 1$ from a total spin-0 to a total spin-1 ground state. In this case the specific heat at low T is given by

$$C \approx x^2 \operatorname{sech}^2(x) \qquad \text{where } x = \frac{(1-B)}{2T} \tag{7}$$

and this is plotted in figure 11.

The double peak is easily understood as occurring at the points where the level separation is of the same order as the temperature. It is closely related to the Schottky anomaly in which the specific heat of a two-level system as a function of temperature has a peak at a temperature corresponding to the level separation.

Also at low temperatures in figure 10 it will be noticed that there appear to be plateaux in the curves between the peaks at $B = 0.8681$, 1.4530 and 2.1327. These are due to very low-lying states with the same S_T^z as the ground state, and the specific heat would also tend to 0 in these regions at very low T.

For $T \gg J$ the system behaves effectively as a set of isolated spins and for N spin-$\frac{1}{2}$ atoms the specific heat is given by

$$C = Nx^2 \operatorname{sech}^2(x) \qquad \text{where } x = \frac{B}{2T} \tag{8}$$

which has a single peak at $x \approx 1.2$, i.e. $B \approx 2.4T$.

The intermediate temperature regime is characterized by a gradual smoothing of the surface as T increases.

Finally we show in figure 12 the $B = 0$ specific heat curves for all clusters with $N \leqslant 13$.

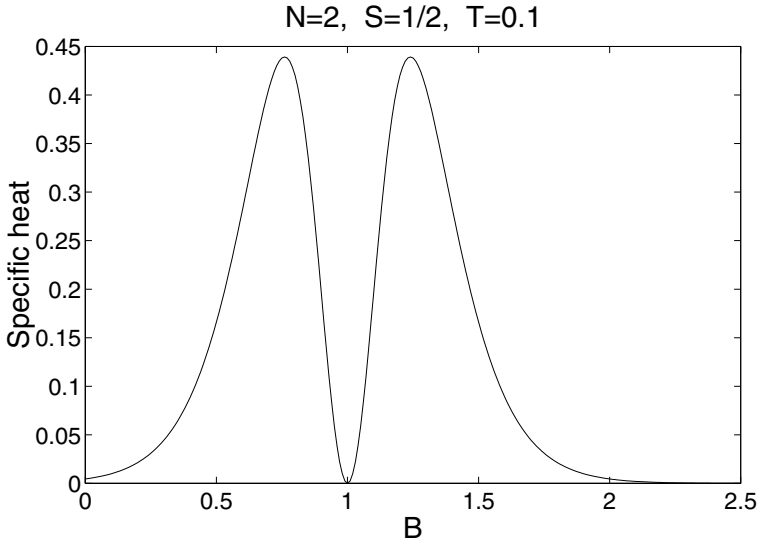

Figure 11. Low-temperature specific heat of a pair of $S = 1/2$ atoms as a function of B.

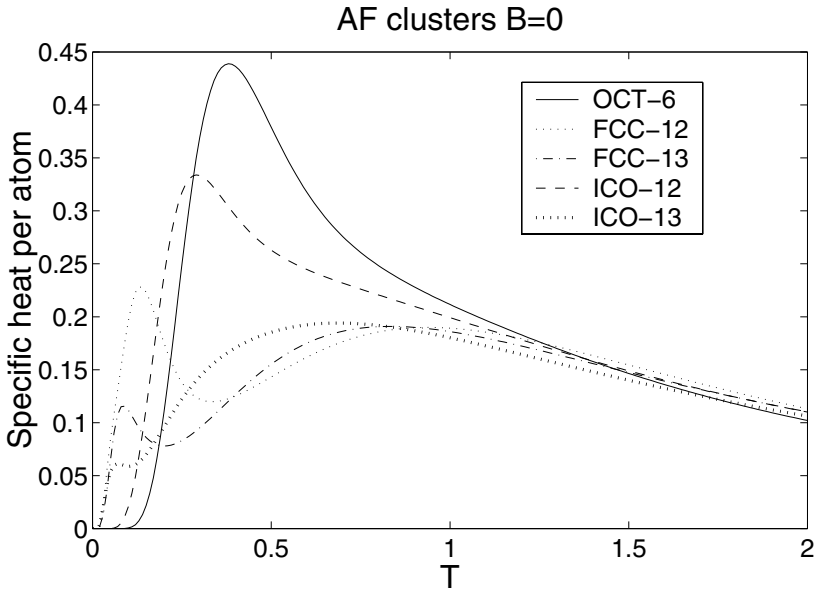

Figure 12. Specific heat curves at $B = 0$.

6. Conclusions

The stepped structure of the magnetization of small clusters as a function of applied magnetic field is qualitatively similar to that previously found for Ising clusters of spins. Heisenberg clusters of spins have more degrees of freedom and for a fixed number of spins there are more distinct energy levels, i.e. less degeneracy. As step widths are related to transitions in the ground state due to level crossings, they are typically smaller for Heisenberg systems.

As very small clusters, exemplified by the octahedron, have simple energy level structures, the resulting magnetization curves have a simple structure of regular steps. For larger clusters the step length shows more variation, but it is difficult to identify any particular pattern, at least for the clusters considered here. Obviously the structures with a central spin show a long plateau before the final step which is related to the rotation of the central spin to be parallel to the applied field. For these small clusters this feature could be used to identify the presence of a structure with such a central spin. For example the FCC-12 and FCC-13 clusters show a very similar behaviour apart from this final step in the latter.

One interesting feature found in the Ising clusters [22] was the appearance of intervals of the applied magnetic field in which magnetization increased with increasing temperature. A similar effect occurs here, but since most of the transitions involve a change of only one unit in the z-component of the angular momentum, the effect is often smaller. Another difference between clusters with an Ising and Heisenberg interactions is that the $T = 0$ magnetization curves in the Ising case are independent of S (with appropriate scaling) and so there are no significant differences between the quantum and classical cases.

The specific heat of spin clusters $C = C(T, B)$ appears to be a convenient way to obtain information about the energy level structure of the quantum systems. At very low temperatures double peaks appear around the applied field values at which there is a level crossing. Each peak corresponds to a 'resonance' between the thermal energy and the level spacing. For increasing temperature the peaks broaden and begin to merge, but even at reasonably high temperature individual peaks can still be distinguished in $C(B)$, i.e. at fixed temperature.

The single dominant peak at high temperature is a precursor of the high-B behaviour. For $B \gg J$ the Zeeman splitting of the levels dominates over the exchange interaction and the cluster behaves effectively as N independent spin-$\frac{1}{2}$ atoms. The position of the single peak is at $B \approx 2.4T$.

On the other hand, if $C(T)$ (fixed B), is considered, the low-temperature structure of this curve depends on the value of B. If B is not close to a $T = 0$ level crossing, then $C = C(T)$ normally shows a monotonic increase for increasing temperature until a broad peak appears which includes contributions from many individual 'thermal resonances'. For an applied field close to a level crossing, and for not too large clusters, one should find a separate peak in $C(T)$ at very low temperatures, resulting from that level crossing, followed later by a broad peak as above. We exemplify this behaviour in figure 12 for $B = 0$. It is evident that for increasing cluster size the plateaux become narrower and contributions from different thermal resonances begin to merge even at very low temperatures.

Study of these magnetic clusters shows that they have an interesting behaviour as a function of magnetic field. The classical clusters show clear transitions between states of different symmetry at certain critical fields. The quantum behaviour is less clear but there is some evidence of similar changes.

We feel that a more detailed analysis of the quantum clusters would be justified. In particular it would be useful to analyse the ground states in terms of the irreducible representations of the point groups of the clusters. This should show whether the $S = \frac{1}{2}$ quantum clusters also have transitions between regions of different symmetry.

Higher-spin quantum clusters would also be interesting, partly because they might be easier to realize experimentally, and partly because they are 'closer' to the classical clusters.

Acknowledgment

We acknowledge useful discussions with R J Elliott.

References

[1] de Heer W A, Milani P and Châtelain A 1990 *Phys. Rev. Lett.* **65** 488
[2] Bucher J P and Bloomfield L A 1993 *Int. J. Mod. Phys.* B **7** 1079
[3] Khanna S N and Linderoth S 1991 *Phys. Rev. Lett.* **67** 742
[4] Merikoski J, Timonen J, Manninen M and Jena P 1991 *Phys. Rev. Lett.* **66** 938
Merikoski J, Timonen J, Manninen M and Jena P 1992 *Physics and Chemistry in Finite Systems: from Clusters to Crystals* ed P Jena, S N Khanna and B K Rao (Amsterdam: Kluwer) pp 785–91
[5] Sessoli R, Gatteschi D, Caneschi A and Novak M A 1993 *Nature* **365** 141
[6] Villain J, Hartmann-Boutron F, Sessoli R and Rettori A 1994 *Europhys. Lett.* **27** 159
[7] Politi P, Rettori A, Hartmann-Boutron F and Villain J 1995 *Phys. Rev. Lett.* **75** 537
[8] Friedmann J R, Sarachik M P, Tejada J and Ziolo R 1996 *Phys. Rev. Lett.* **76** 3830
[9] Thomas L, Lionti F, Ballou R, Gatteschi D, Sessoli R and Barbara B 1996 *Nature* **383** 145
[10] Fort A, Rettori A, Villain J, Gatteschi D and Sessoli R 1998 *Phys. Rev. Lett.* **80** 612
[11] Katsnelson M I, Dobrovitski V V and Harmon B N 1999 *Phys. Rev.* B **59** 6919
[12] Leuenberger M N and Loss D 1999 *Europhys. Lett.* **46** 692
Leuenberger M N and Loss D 2000 *Phys. Rev.* B **61** 1286
[13] Barra A-L, Debrunner P, Gatteschi D, Schulz Ch E and Sessoli R 1996 *Europhys. Lett.* **35** 133
[14] Sangregorio C, Ohm T, Paulsen C, Sessoli R and Gatteschi D 1997 *Phys. Rev. Lett.* **78** 4645
[15] Ohm T, Sangregorio C and Paulsen C 1998 *Eur. Phys. J.* B **6** 595
[16] Wernsdorfer W and Sessoli R 1999 *Science* **284** 133
[17] Leuenberger M N and Loss D 2000 *Phys. Rev.* B **61** 12 200
[18] Jensen P J and Bennemann K H 1995 *Z. Phys.* D **35** 273
[19] Bouarab S, Vega A, López M, Iñiguez M P and Alonso J A 1997 *Phys. Rev.* B **55** 13 279
[20] Muñoz-Sandoval E, Dorantes-Dávila J and Pastor G M 1999 *Eur. Phys. J.* D **5** 89
[21] Viitala E, Häkkinen H, Manninen M and Timonen J 2000 *Phys. Rev.* B **61** 8851
[22] Viitala E, Merikoski J, Manninen M and Timonen J 1997 *Z. Phys.* D **40** 173
Viitala E, Merikoski J, Manninen M and Timonen J 1997 *Phys. Rev.* B **55** 11 541
[23] *Numerical Recipes* 1986 (Cambridge: Cambridge University Press) ch 10